ACS APPLIED MATERIALS & INTERFACES

Research Article

www.acsami.org

Tunable White-Light-Emitting Mn-Doped ZnSe Nanocrystals

Vijay Kumar Sharma,[†] Burak Guzelturk,[†] Talha Erdem,[†] Yusuf Kelestemur,[†] and Hilmi Volkan Demir*[,†,‡]

[†]UNAM—Institute of Materials Science and Nanotechnology, Department of Electrical and Electronics Engineering, and Department of Physics, Bilkent University, Ankara 06800, Turkey

[‡]Luminous! Center of Excellence for Semiconductor Lighting and Displays, School of Electrical and Electronic Engineering, and School of Mathematical and Physical Sciences, Nanyang Technological University, Singapore 639798, Singapore

Supporting Information

ABSTRACT: We report white-light-emitting Mn-doped ZnSe nanocrystals (NCs) that are synthesized using modified nucleation doping strategy. Tailoring three distinct emission mechanisms in these NCs, which are MnSe-related blue emission (410 and 435 nm), Zn-related defect state green emission (520 nm), and Mn-dopant related orange emission (580 nm), allowed us to achieve excitation wavelength tailorable white-light generation as studied by steady state and time-resolved fluorescence spectroscopy. These NCs will be promising as single component white-light engines for solid-state lighting.

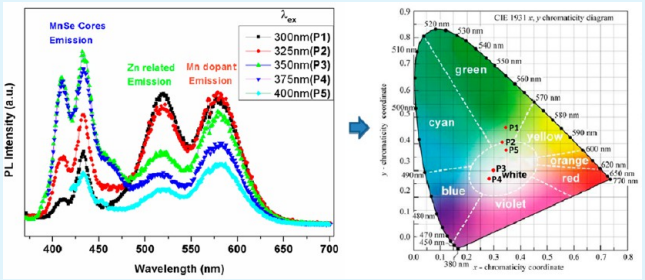

KEYWORDS: *doped nanocrystals, white-light emission, transmission electron microscopy, time-resolved photoluminescence, color properties*

1. INTRODUCTION

White-light emission (WLE) from nanocrystals (NCs)[1] is presently a research area of intense interest, especially for the purpose of generation of photometrically high quality white light while maintaining the energy efficiency for solid-state lighting. One of the most common ways to generate white-emitting NC-based phosphors is to combine red-, green-, and blue-emitting NCs in an appropriate ratio.[1,2] However, when one simply mixes together the NCs of different color emission to generate white light, these systems suffer from various drawbacks including self-absorption by the small-bandgap NCs, scattering of the light at the boundaries of color conversion layers, and undesired nonradiative energy transfer among the nanoemitters.[3] This also contributes to undesirable changes in the chromaticity coordinates and photometric performance of the light-emitting diodes (LEDs) due to the different relative temporal stabilities of the components of the white-LEDs.[4] Current research on white-light emission has heavily focused on cadmium based NCs (e.g., by mixing red, green, and blue light from core NCs such as CdS, CdSe, CdTe, or core/shell NCs including CdSe/ZnS and CdSe/CdS)[5−7] and magic-sized CdSe NCs.[8] Recently, Rosson et al.[9] reported a bright white-light emission from ultrasmall CdSe nanocrystals treated with carboxylic acids. However, due to the intrinsic toxicity of cadmium, the long-term practical applications of Cd-based NCs have been forecasted to be limited.[10] Therefore, single-component white-light generating NCs are highly desirable and gaining increasingly more importance in the recent years. These single component white light emitters could address the issues that have been mentioned above, along with the potential to improve the color stability, to reduce the device complexity and to lower the cost as compared to utilizing multi-NC-based color conversion layers for white-LEDs. To this end, Mn-doped NCs (e.g., ZnSe,[11−13] ZnS,[14,15] CdS,[16] etc.) are considered to be potential candidates as single white-light generating phosphors avoiding the issues of toxicity and self-absorption. Mn-doped ZnSe NCs were already reported as white-light generating nanophosphors. For the means of achieving WLE, tuning of Mn-dopant concentration along with the wide band-edge emission from the semiconductor host was utilized, surface modification (i.e., surface-chelating) was employed to create blue-green emitting surface states, co-doping of the NCs with other dopants such as Cu was proposed,[4] and hybridization with organic molecules was demonstrated.[17] However, in all of the previous reports, the tunability of WLE from the Mn-doped NCs has not been possible, and the temporal stability of the WLE states was poor and depended on environmental conditions.[4,11] In this paper, we report the generation of WLE from Mn-doped ZnSe NCs that is achieved via utilization of three distinct emission states in these NCs, which are here shown to be tunable as controlled during the synthesis of these NCs. These three distinct emission states are MnSe-related blue emission at 410 and 435 nm, Zn-related green emission at 520 nm, and Mn-dopant-related orange emission at 580 nm. Furthermore, we have shown that, by employing these distinct states that have different photo-

Received: December 26, 2013
Accepted: February 6, 2014
Published: February 6, 2014

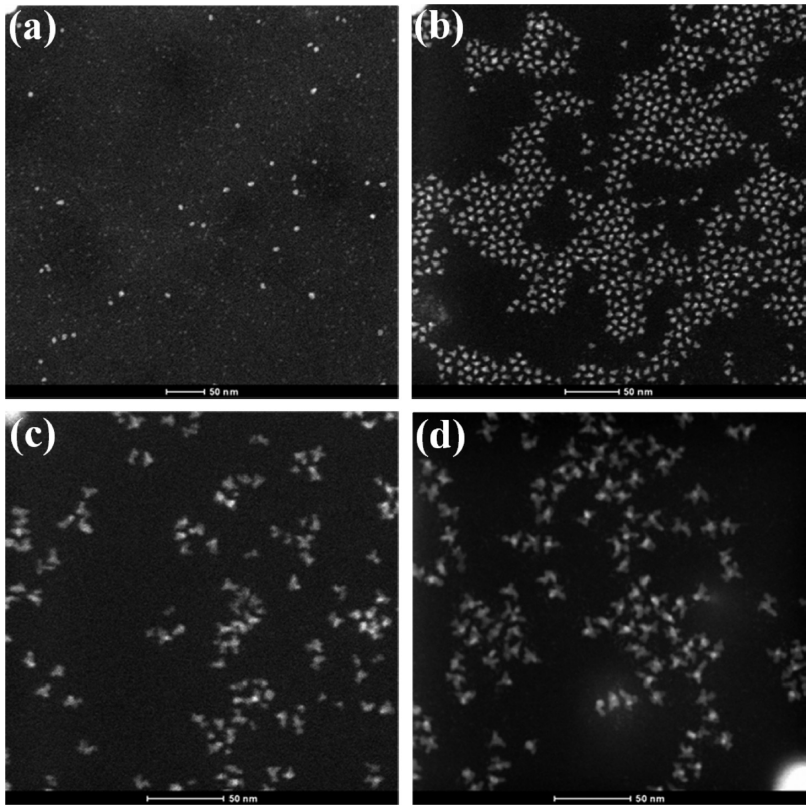

Figure 1. HAADF-STEM images of (a) MnSe cores and Mn-doped ZnSe NCs obtained after the (b) first, (c) second, and (d) third injections of Zn precursor. The scale bars are 50 nm.

luminescence excitation spectra, WLE can be tailored by changing the wavelength of the excitation source. Here, we show that, by tuning the excitation wavelength from 325 to 400 nm, different shades of white light can be reproducibly generated, which is technologically promising for solid-state lighting. To the best of our knowledge, this type of tunable WLE from monoemitter Mn-doped ZnSe NCs has not been reported earlier.

2. EXPERIMENTAL SECTION

Mn-doped ZnSe NCs are synthesized using nucleation doping strategy[10] with slight modifications to obtain white light, and the NCs are purified using a new methodology as described in detail in the Supporting Information. UV−vis spectra were obtained using a UV−vis spectrophotometer (Varian - Cary 100). Photoluminescence (PL) spectra (both excitation and emission) of the NCs were obtained with a fluorescence spectrophotometer (Varian - Cary Eclipse). The quantum yield of the NCs was measured using Horiba Jobin Yvon Time resolved fluorescence setup using an integrating sphere F-3018. The time-resolved fluorescence measurements were taken with a Pico Quant Fluo Time 200 setup using an excitation wavelength of 375 nm. HAADF-STEM and HR-transmission electron microscopy (TEM - Tecnai G2 F30) images were obtained using TEM operating at 300 kV. Elemental analysis was carried out using energy dispersive X-ray spectroscopy (EDS).

3. RESULTS AND DISCUSSION

Transmission electron microscopy (TEM) was performed to understand the morphology and crystal structure of the Mn-doped ZnSe NCs. Figure 1 shows high-angle annular dark-field (HAADF) scanning transmission electron microscope (STEM) images of Mn-doped ZnSe NCs obtained after the first, second, and third injections of Zn precursor on the MnSe cores. Figure 1a shows HAADF-STEM images of MnSe cores with two different sizes of ∼2 and 4 nm, both having a spherical geometry. Almost 90% of the NCs are of small size (i.e., 2 nm), and the rest are bigger NCs (i.e., 4 nm) as observed from the zoomed in image of MnSe cores, as shown in Figure S1 of the Supporting Information. Figure 1b shows Mn-doped ZnSe NCs obtained after first injection of Zn precursor, exhibiting an average size ∼4.8 nm with a nearly spherical (i.e., tetrapod with very short branches) shape. As the number of Zn precursor injections is increased, the shape of the NCs deviates from nearly spherical to branched. The branched Mn-doped ZnSe NCs obtained after the third injection of Zn precursor have a uniform size of ∼9.5 nm, with a core diameter of ∼4.3 nm and a branch length of ∼5.2 nm. The number of NCs with a tetrapod shape is almost 95%; there are also some bipods, as seen in Figure 1c. There are few reports on the shape control of Mn-doped ZnSe NCs.[18,19] Peng et al.[19] synthesized both branched and spherical Mn-doped ZnSe NCs by tuning the ratio of fatty acids and fatty amines. They observed that both the branches and the core crystallize in the zinc blende structure. We also carried out a detailed HR-TEM investigation to understand the growth mechanism of our branched Mn-doped ZnSe NCs. The HR-TEM images of Mn-doped ZnSe NCs obtained after the (a) first (nearly spherical NCs) and (b) third (branched NCs) injections of Zn precursor are shown in Figure S2 of Supporting Information. For nearly spherical Mn-doped ZnSe NCs, the interplanar spacing obtained is ∼3.26 Å (Figure S2a), which corresponds to the (111) plane of zinc blende (ZB) structure and lies between ∼3.36 Å (MnSe cores) (JCPDS 73-1742) and ∼3.24 Å (ZnSe) (JCPDS 80-0021). The value is closer to that of the ZnSe ZB structure because of the thicker ZnSe shell over MnSe core. These results were further

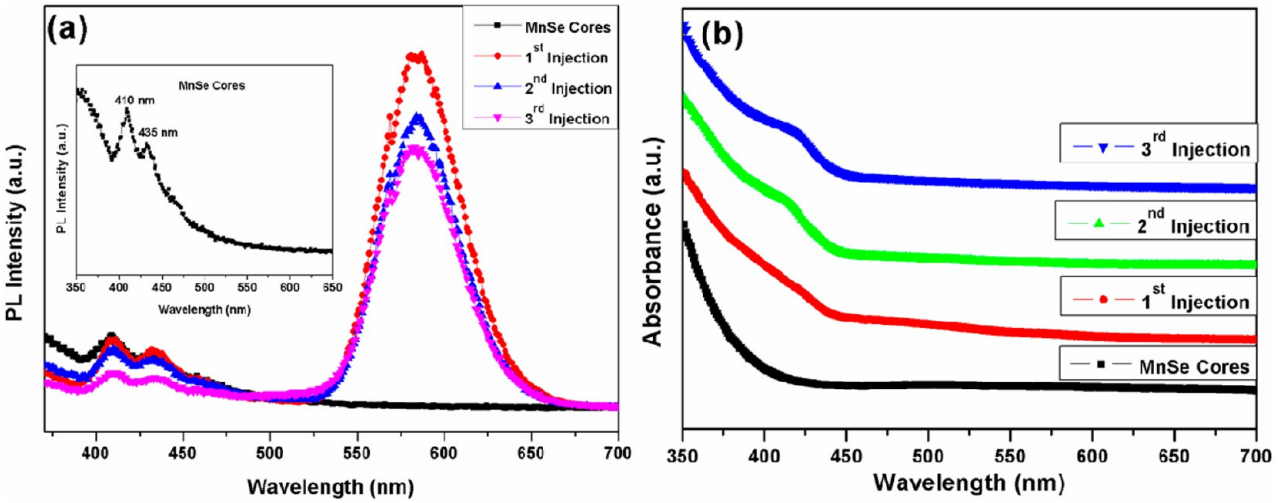

Figure 2. PL (a) and absorption spectra (b) of MnSe cores and Mn-doped ZnSe NCs obtained after first, second, and third injections of Zn precursor. In the inset of part a, the zoomed in PL spectra of MnSe cores are shown for clarity. PL spectra are recorded at an excitation wavelength of 300 nm for all cases.

verified by energy dispersive X-ray spectroscopy (EDS). For the branched Mn-doped ZnSe NCs, the interplanar *d* spacing obtained from the branches is ~3.49 Å (Figure S2b). This value corresponds to the (100) plane of wurtzite ZnSe having a standard value ~3.44 Å (JCPDS 80-0008). Therefore, in our case, we observe that the core crystallizes in the zinc blende structure, whereas the branches crystallize in the wurtzite structure. Furthermore, we observed the transformation from nearly spherical to branch NCs after the second injection of Zn precursor on the MnSe core, with no variation in stearic acid concentration, which is in contrast to ref 19. Recently, Wu and Warner[18] reported shape control of Mn-doped ZnSe NCs by varying Zn precursor and the temperature of the injection (i.e., $ZnSt_2$/290 °C/branched NCs and $ZnCl_2$/220 °C/spherical NCs). But the maximum photoluminescence quantum efficiency reported for the branched NCs remained only at 1%; in contrast, here we report an efficiency of 13.6% for the branched Mn-doped ZnSe NCs. The detailed elemental analysis done by using EDS also supports the growth mechanism revealed by HR-TEM data. The elemental concentration obtained for the spherical NCs is Mn = 1.39 atom %; Zn = 56.22 atom %; and Se = 42.37 atom %, whereas for the branched NCs the values are Mn = 1.20 atom %; Zn = 66.36 atom %; and Se = 32.43 atom %. As the number of Zn precursor injections is increased, the Zn content is enhanced in the NCs as expected. Using EDS, Mn was detected only in the core area of the branched Mn-doped ZnSe NCs. The HR-TEM and elemental analysis of Mn-doped ZnSe NCs suggested that, in our case, the proposed atomic model for the branched Mn-doped ZnSe NCs structure consists of zinc blende (111) plane of ZnSe core jointly with wurtzite (100) plane of ZnSe arms, Mn atoms being embedded in the core only.[20]

The photoluminescence (PL) spectra of MnSe cores and Mn-doped ZnSe NCs obtained after the first, second, and third injections of Zn precursor excited at 300 nm are shown in Figure 2a. PL spectra of Mn-doped ZnSe NCs were dominated by the Mn dopant emission at 580 nm, accompanied with two weak emissions at 410 and 435 nm. Mn-doped emission at 580 nm is independent of the shape of Mn-doped ZnSe NCs with a fwhm of 52 (± 1) nm. For the emission of the Mn dopant, we observe a decrease in the PL intensity with the increasing number of Zn precursor injections on the MnSe core. The decrease in the PL intensity can be accounted for by the deviation in shape from the spherical to the branched with the increasing number of Zn precursor injections. This change in the PL behavior is analyzed and verified with the structural features of our Mn-doped ZnSe NCs (Figure 1). These results are consistent with the previous reports.[18,19] A gradual red shift in the excitonic absorption band from 410 to 420 nm is observed in the UV−vis absorption spectra with increasing the number of Zn precursor injections, as shown in Figure 2b. While considering the Mn-dopant emission at 580 nm, the Stokes shift of ~160−170 nm is achieved as compared with the first exciton absorption peak of the ZnSe NCs. In Figure 2a, the emission peaks at 410 and 435 nm are observed for all the samples. These blue emission peaks are attributed to the MnSe core of the Mn-doped ZnSe NCs. This is substantiated by measuring the PL spectra of the only MnSe cores that were used as the seed for the Mn-doped ZnSe NCs as shown in the inset of Figure 2a.

The UV−vis spectrum of the MnSe cores does not show any observable features at visible wavelengths up to the UV region (350 nm) in accordance with the previous study.[10] On the basis of the UV−vis data, the optical band gap (E_g) was estimated to be approximately 3.5−3.8 eV. This value is significantly larger than that for rocksalt-type MnSe (E_g ~ 2.5 eV)[21] but is consistent with the band gap of ZB-type MnSe (E_g ~ 3.4 eV).[22] This observation is also supported by the HR-TEM analysis of the ZB-type MnSe core as discussed above. HR-TEM image of the MnSe core is shown in the inset of Figure S1 of the Supporting Information. In the PL spectrum, there are two observable emission peaks at ~410 and 435 nm. Since the characteristic emission peaks do not belong to octahedrally and tetrahedrally coordinated MnSe,[23] these vibronic-like emission peaks possibly originate from the defects in the NC cores, presumed to be caused by the metastability of MnSe in the zinc blende structure. The exact origins of these emissions are, however, not clear. Similar emissions were also reported by Zhu et al.[24] from the ZB-type MnSe cores while studying MnSe/CdSe core shell nanocrystals.

In our Mn-doped ZnSe NCs PL spectra (Figure 2a), we observe emissions both from Mn-dopant and MnSe cores,

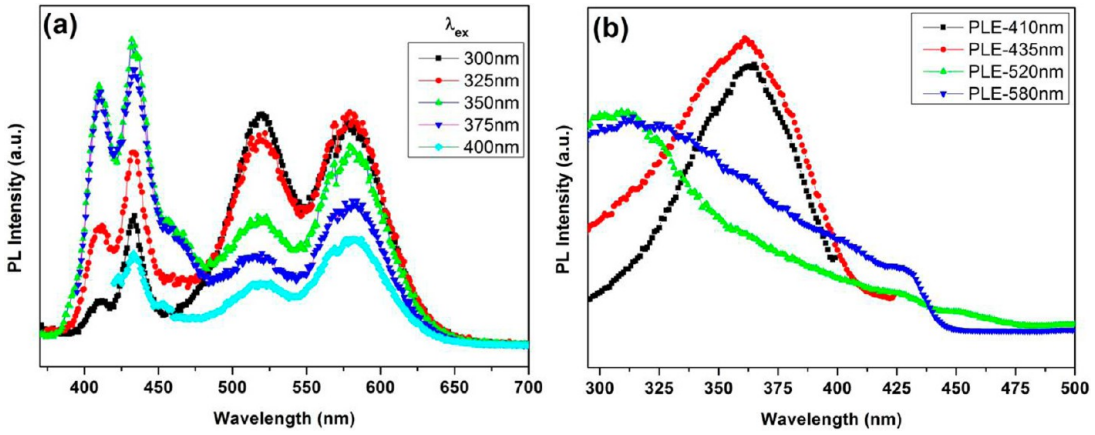

Figure 3. (a) PL spectra of the modified Mn-doped ZnSe NCs under excitation at various wavelengths. (b) PLE spectra of all emissions in Mn-doped ZnSe NCs.

simultaneously. These emissions cannot be explained by nucleation doping strategy alone. In our case, on the basis of optical and structural characterization, there are two possible reasons for these emissions. First, there is a possibility that, rather than a nucleation doping synthesis, in our case we have a two-step nucleation synthesis. In a two-step nucleation model, the amorphous polynuclei or polymolecules aggregate together in the first step, and in the second step, these amorphous structures start to adjust the positions of atoms and reorganize these clusters into the crystalline form.[25] If two regions on the surface crystallize at the same time in the second step of surface nucleation, then they could not fuse into one single crystal and a twin boundary is formed. We also observed twinning in our synthesized Mn-doped ZnSe NCs as shown in Figure S3 of Supporting Information. For a second possibility, in our synthesis we found MnSe cores of two sizes with 90% of the MnSe cores being smaller (2 nm) and the remaining being larger (4 nm). By coating these NCs with ZnSe, the smaller and bigger MnSe cores both lead to Mn-doped ZnSe NCs but with thicker and thinner ZnSe shells, respectively. For the thinner shells there are emissions from MnSe cores, too. This hypothesis is also supported by the PL spectra in Figure 2a; as the ZnSe coating on MnSe core increases, the intensity of emission from MnSe cores decreases. PL spectra of Mn-doped ZnSe NCs normalized at 580 nm also support our hypothesis as shown in the Figure S4 of Supporting Information. Also, it is observed that as we increase the concentration of Mn in the synthesis the intensity of the PL emission (410 and 435 nm) from the MnSe cores increases, which is not shown here. Therefore, in our case we have emissions both from Mn-dopant and MnSe cores simultaneously for the Mn-doped ZnSe NCs.

In this study, we further utilize Mn-doped ZnSe NCs as monoemitter WLE agents. In addition to the blue emission from MnSe cores and the orange emission from Mn-dopant, a green emission was required to achieve high-quality white light. By tuning the zinc stearate to stearic acid ratio simultaneously with the Zn to Se ratio, we were able to obtain the green emission in addition to the blue and orange emission using a modified recipe (hereafter called as modified synthesis, described in detail in the Experimental Section). Thus, the white light generation was realized from the modified synthesis of Mn-doped ZnSe NCs as a result of the combination of light emission in orange (Mn-dopant emission), in green (Zn related defects), and in blue (MnSe cores emission) simultaneously. These three emissions can be controlled to achieve high-quality white light. The modified Mn-doped ZnSe NCs demonstrated excitation wavelength dependent emission color tunability, which was studied at room-temperature as shown in Figure 3a. The HAADF-STEM images of these NCs obtained using the modified synthesis exhibits tetrapode shape with an average size ~8.5 nm as shown in Figure S5 of the Supporting Information.

We observe that PL spectra obtained from the modified synthesis of Mn-doped ZnSe NCs shows four emission peaks; two blue emission peaks at 410 and 435 nm, one green emission peak at 520 nm, and one orange emission peak at 580 nm. The blue emission peaks at 410 and 435 nm are the emissions from MnSe cores as discussed above. The green emission around 520 nm is attributed to "self-activated" luminescence, as a consequence of donor−acceptor pairs that are related to Zn vacancy and crystal defects (interstitial states or associated with dislocations, stacking faults, and non-stoichiometric defects).[26,27] The green band is observed in the samples annealed in Zn vapor, vacuum, or reducing atmosphere, resulting in Zn excess.[28] Green emission was also reported in both undoped and Mn doped ZnS nonorods by Biswas et al.,[29] and they concluded that this emission is due to zinc-vacancy related defect states. Our samples were grown in Zn-rich conditions; thus, we believe that the strong emission may be ascribed to the interstitial Zn defect and non-stoichiometric defects. The orange emission at 580 nm is due to the $^4T_1-^6A_1$ transition of the Mn impurity excited by energy transfer from the ZnSe lattice.

To investigate the origin of these emission bands, PLE spectra of Mn-doped ZnSe NCs were recorded. Figure 3b shows the PLE spectra for the emission at 410, 435, 520, and 580 nm. The PLE peak position for the 580 nm emission wavelength is 310 nm, indicating that the orange emission is from Mn-doped ZnSe NCs.[10] PLE spectra of the orange emission have a bump at 430 nm, which is similar to the first exciton peak in the absorption spectra of Mn-doped ZnSe NCs shown in Figure S6 of Supporting Information. We observed that in this case the absorption peak is 10 nm red-shifted in comparison to the branched one due to thicker ZnSe coating. In contrast, the PLE spectrum recorded for the 520 nm emission exhibits a maxima at 310 nm along with a shoulder bumping at 360 nm. The 360 nm PLE peak is associated with Zn-related defects as reported previously.[30] The green emission observed at 520 nm, which is new in our case, is attributed to

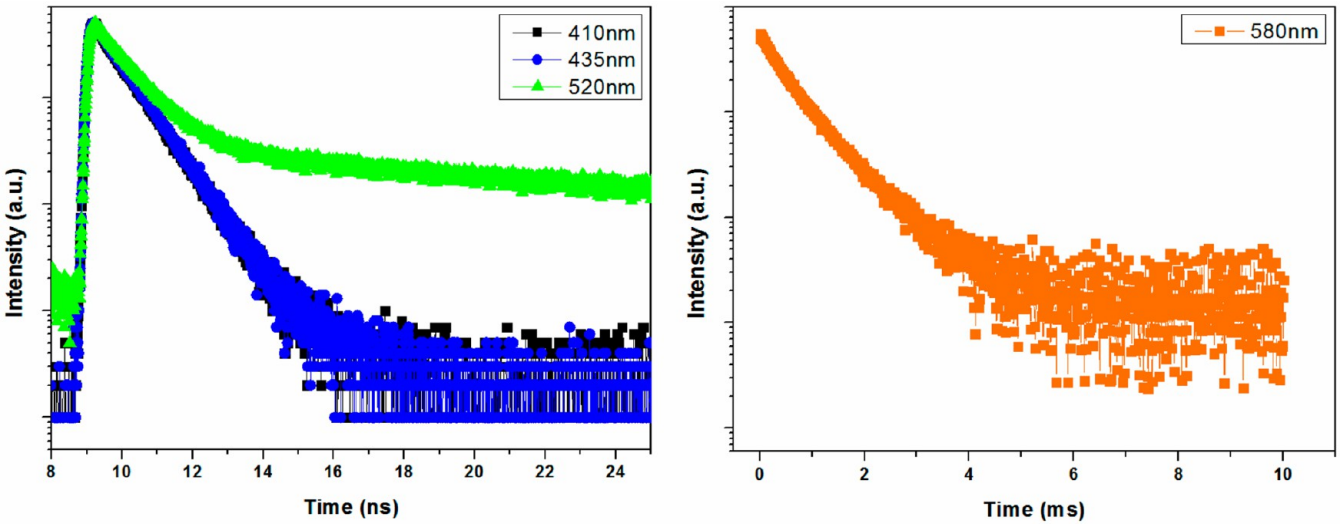

Figure 4. TRPL spectroscopy of Mn-doped ZnSe NCs.

the modified synthesis of these NCs. Thus, the green emission is due to zinc related defects (excess Zinc) in the Mn-doped ZnSe NCs.[28] The green emission (520 nm) has a maximum at 310 nm, but immediately afterward the emission decreases with increasing wavelength. Thus, the green emission is not related to Mn-doping in ZnSe. Also, in Figure 3b, we have recorded PLE plots for 410 and 435 nm, both having their maximum at 365 nm. After 330 nm the blue emission (410 and 435 nm) starts to increase and reaches its maximum at 365 nm. Thus, PLE results indicate that all these emissions have different origins which are further confirmed via time-resolved photoluminescence (TRPL) spectroscopy.

Figure 4 shows the fluorescence decay curves for all four (410, 435, 520, and 580 nm) emissions of Mn-doped ZnSe NCs excited at 375 nm. The PL decay profile of the orange emission (580 nm) is found to be single exponential with an average lifetime of 0.59 ms. Such a slow decay further confirmed the attribution of this emission band to the spin forbidden doped Mn^{2+} $^4T_1$ to $^6A_1$ transition. Then, we studied the emission kinetics for the blue emission at wavelengths of 410 and 435 nm, which exhibited a single exponential decay with fast emission decay lifetimes of 0.61 and 0.63 ns, respectively. Generally for semiconductor NCs, the fluorescence lifetimes are of the order of a couple of nanoseconds or longer; thus, these fast decay kinetics for the blue emission at 410 and 435 nm (arising from MnSe cores emission) is due to trap state emission of the MnSe cores together with possible competition with other nonradiative channels such that overall PL decay lifetime is quite short, or the other explanation to these vibronic-like blue emissions would be the formation of very small MnSe nanoclusters. Having similar lifetimes for 410 and 435 nm indicates that there exists excitons which are highly bound to each other (similar to Frenkel excitons rather than Wannier-Mott excitons) since the MnSe core is too small (like a nanocluster) before the ZnSe shell growth. Also, these two emission states were observed from the steady state PL of only MnSe cores (Figure 2b). Also, relatively good PL QY of these blue emission states supports the fact that nonradiative decay channels cannot be highly dominant. Moreover, PLE of these states (see Figure 3b) has a resonance feature around 365 nm that supports the hypothesis that the blue emission is more likely to be arising from the MnSe nanoclusters rather than highly inefficient trap states.

For the green emission at 520 nm, the average lifetime of 1.72 ns is obtained, which is attributed to zinc related defects introduced in our system by the modified synthesis. The value 1.72 ns is the amplitude weighted average lifetime of the 520 nm emission obtained after fitting the curve with three exponentials (reduced $\chi^2 \sim 1$). These lifetime components are 0.804 ns (92.96%), 3.74 ns (3.37%), and 23.02 ns (3.67%). The fastest lifetime component is attributed to the direct recombination lifetime of the 520 nm emission state. Longer lifetime components may be related to the shallow trap state mediated emission causing a delayed emission with longer fluorescence lifetime components.[31] There is a possibility that, since the sample has excess Zn, the cleaning process may produce some oxidized Zn, which may be a reason for the green emission in PL.[32] The lifetime of the green emission is slower than the blue emission and much faster than the orange emission suggesting that these three emission states are distinct and have different emission mechanisms that are independently controlled as shown by PLE spectra in Figure 3b. Therefore, the above results indicate that, by controlling the synthesis parameters, we can tune the WLE from the Mn-doped ZnSe NCs, thus making it possible to be used as versatile monoemitters for WLE. The intensity of these relative emissions can be tuned by varying the excitation wavelengths; thus, white light generation can be easily controlled and tuned.

Figure 5 shows the chromaticity coordinates of the emission from modified Mn-doped ZnSe NCs excited at 300 nm (P1), 325 nm (P2), 350 nm (P3), 375 nm (P4), and 400 nm (P5), where these different excitation wavelengths lead to chromaticity coordinates of (0.34, 0.46), (0.33, 0.40), (0.30, 0.30), (0.28, 0.26), and (0.34, 0.37), respectively. The photometric color properties (LER, CCT, CRI) are calculated for all excitation wavelengths and are listed in Table 1. Here the chromaticity coordinates corresponding to the excitation wavelengths 325, 350, 375, and 400 nm fall within the white region of the 1931 CIE (Commission Internationale de L'Eclairaged) diagram[33] (Figure 5). Through excitation source tuning, white light from the NCs can be tuned to its different shades with luminous efficacy up to 400 lm/W and correlated color temperature in the range of 5000−11000 K. Therefore,

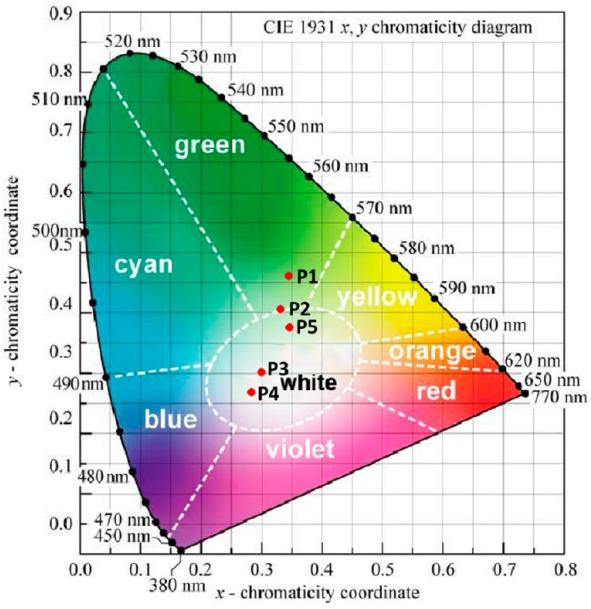

Figure 5. CIE chromaticity diagram for Mn-doped ZnSe NCs.

Table 1. Color Properties of Mn-Doped ZnSe NCs

λ_{ex} (nm)	(x, y)	LER (lm/W_{opt})	CCT (K)	CRI
300 (P1)	(0.3456, 0.4615)	401	5213	48
325 (P2)	(0.3311, 0.4057)	354	5556	51
350 (P3)	(0.2993, 0.3010)	265	7769	60
375 (P4)	(0.2834, 0.2677)	236	11170	64
400 (P5)	(0.3458, 0.3758)	357	5049	50

WLE with high color quality is successfully achieved for Mn-doped ZnSe NCs.

4. CONCLUSIONS

In this paper, we report WLE from the Mn-doped ZnSe NCs that are synthesized with a modified synthesis reported here. As a result, we achieve three controllable distinct emission states from these NCs; blue emission from the MnSe cores, orange emission from the Mn dopant, and green emission from the Zn-related defect states. All these emissions are reproducibly controlled by small variation in the synthesis parameters. The tailoring of the white emission via excitation source wavelength owing to the distinct PLE characteristics of the three emission states enabled us to tune the white light from the same NCs for the first time in the literature. These Mn-doped ZnSe NCs are promising as versatile light emitting materials suitable for various applications ranging from solid-state lighting to bioimaging.

■ ASSOCIATED CONTENT

Supporting Information

HAADF-STEM and HR-TEM images of MnSe cores (Figure S1); HR-TEM images of Mn-doped ZnSe NCs obtained after the (a) first and (b) third injections of Zn precursor (Figure S2); HR-TEM image of Mn-doped ZnSe NCs showing twin boundary (Figure S3); PL spectra of Mn-doped ZnSe NCs obtained after the first, second, and third injections of Zn precursor normalized at 580 nm (Figure S4); HAADF-STEM image of the Mn-doped ZnSe NCs that generates white light (Figure S5); absorption spectra of Mn-doped ZnSe NCs that generates white light (Figure S6). This material is available free of charge via the Internet at http://pubs.acs.org.

■ AUTHOR INFORMATION

Corresponding Author

*(H.V.D.) E-mail: volkan@bilkent.edu.tr. Tel.:+90312-290-1021.

Notes

The authors declare no competing financial interest.

■ ACKNOWLEDGMENTS

This work is supported by EU-FP7 Nanophotonics4Energy NoE and TUBITAK EEEAG, 110E217. H.V.D. gratefully acknowledges ESF-EURYI and TUBA-GEBIP. T.E. and Y.K. acknowledge TUBITAK fellowship.

■ REFERENCES

(1) Erdem, T.; Demir, H. V. Color science of nanocrystal quantum dots for lighting and displays. *Nanophotonics* **2013**, *2*, 57−81.
(2) Ali, M.; Chattopadhyay, S.; Nag, A.; Kumar, A.; Sapra, S.; Chakraborty, S.; Sarma, D. D. White-light emission from a blend of CdSeS nanocrystals of different Se:S ratio. *Nanotechnology* **2007**, *18*, 075401.
(3) Roushan, M.; Zhang, X.; Li, J. Solution-Processable White-Light-Emitting Hybrid Semiconductor Bulk Materials with High Photoluminescence Quantum Efficiency. *Angew. Chem.* **2012**, *124*, 451−454.
(4) Panda, S. K.; Hickey, S. G.; Demir, H. V.; Eychmuller, A. Bright White-Light Emitting Manganese and Copper Co-Doped ZnSe Quantum Dots. *Angew. Chem., Int. Ed.* **2011**, *50*, 4432−4436.
(5) Lita, A.; Washington, A. L., II; van de Burgt, L.; Strouse, G. F.; Stiegman, A. E. Stable Efficient Solid-State White-Light-Emitting Phosphor with a High Scotopic/Photopic Ratio Fabricated from Fused CdSe-Silica Nanocomposites. *Adv. Mater.* **2010**, *22*, 3987−3991.
(6) Lee, J.; Sundar, V. C.; Heine, J. R.; Bawendi, M. G.; Jensen, K. F. Full Color Emission from II-VI Semiconductor Quantum Dot-Polymer Composites. *Adv. Mater.* **2000**, *12*, 1102−1105.
(7) Demir, H. V.; Nizamoglu, S.; Erdem, T.; Mutlugun, E.; Gaponik, N.; Eychmuller, A. Quantum dot integrated LEDs using photonic and excitonic color conversion. *Nano Today* **2011**, *6*, 632−647.
(8) Bowers, M. J., II; McBride, J. R.; Rosenthal, S. J. White-Light Emission from Magic-Sized Cadmium Selenide Nanocrystals. *J. Am. Chem. Soc.* **2005**, *127*, 15378−15379.
(9) Rosson, T. E.; Claiborne, S. M.; McBride, J. R.; Stratton, B. S.; Rosenthal, S. J. Bright White Light Emission from Ultrasmall Cadmium Selenide Nanocrystals. *J. Am. Chem. Soc.* **2012**, *134*, 8006−8009.
(10) Pradhan, N.; Peng, X. Efficient and Color-Tunable Mn-Doped ZnSe Nanocrystal Emitters: Control of Optical Performance via Greener Synthetic Chemistry. *J. Am. Chem. Soc.* **2007**, *129*, 3339−3347.
(11) Shao, P.; Wang, H.; Zhang, Q.; Li, Y. White light emission from Mn-doped ZnSe d-dots synthesized continuously in microfluidic reactors. *J. Mater. Chem.* **2011**, *21*, 17972−17977.
(12) Lee, S. M.; Hwang, C. S. Synthesis of a White-Light-Emitting ZnSe:Mn Nanocrystal via Thermal Decomposition Reaction of Organometallic Precursors. *Bull. Korean Chem. Soc.* **2013**, *34*, 321−324.
(13) Yang, B.; Zhang, J.; Cui, Y.; Wang, K. White light-emitting diode coated with ZnSe:Mn/ZnSe nanocrystal films enveloped by SiO_2. *Appl. Opt.* **2011**, *50*, G137−G141.
(14) Quan, Z.; Yang, D.; Li, C.; Kong, D.; Yang, P.; Cheng, Z.; Lin, J. Multicolor Tuning of Manganese-Doped ZnS Colloidal Nanocrystals. *Langmuir* **2009**, *25*, 10259−10262.
(15) Kar, S.; Biswas, S. White Light Emission from Surface-Oxidized Manganese-Doped ZnS Nanorods. *J. Phys. Chem. C* **2008**, *112*, 11144−11149.

(16) Nag, A.; Sarma, D. D. White Light from Mn^{2+}-Doped CdS Nanocrystals: A New Approach. *J. Phys. Chem. C* **2007**, *111*, 13641−13644.
(17) Wu, P.; Yan, X. P. Doped quantum dots for chemo/biosensing and bioimaging. *Chem. Soc. Rev.* **2013**, *42*, 5489−5521.
(18) Wu, Y. A.; Warner, J. H. Shape and property control of Mn doped ZnSe quantum dots: from branched to spherical. *J. Mater. Chem.* **2012**, *22*, 417−424.
(19) Viswanatha, R.; Battaglia, D. M.; Curtis, M. E.; Mishima, T. D.; Johnson, M. B.; Peng, X. Shape Control of Doped Semiconductor Nanocrystals (d-Dots). *Nano Res.* **2008**, *1*, 138−144.
(20) Manna, L.; Milliron, D. J.; Meisel, A.; Scher, E. C.; Alivisatos, A. P. Controlled growth of tetrapod-branched inorganic nanocrystals. *Nat. Mater.* **2003**, *2*, 382−385.
(21) Kan, S.; Felner, I.; Banin, U. Synthesis, Characterization, and Magnetic Properties of α-MnS Nanocrystals. *Isr. J. Chem.* **2001**, *41*, 55−61.
(22) Ishibe, I.; Nabetani, Y.; Kato, T.; Matsumoto, T. MBE growth and RHEED characterization of MnSe/ZnSe superlattices on GaAs (100) substrates. *J. Cryst. Growth* **2000**, *214/215*, 172−177.
(23) Heimbrodt, W.; Goede, O.; Tschentscher, I.; Weinhold, V.; Klimakow, A.; Pohl, U.; Jacobs, K.; Hoffmann, N. Optical study of octahedrally and tetrahedrally coordinated MnSe. *Physica B* **1993**, *185*, 357−361.
(24) Zhu, K.; Zhang, X.; Wang, L.; Zhang, H.; Wei, J.; Wang, L.; Zhou, M.; Feng, B. Manganese-doped MnSe/CdSe core/shell nanocrystals: Preparation, characterization, and study of growth mechanism. *J. Mater. Res.* **2011**, *26*, 2400−2406.
(25) Bryan, J. D.; Gamelin, D. R. Doped Semiconductor Nanocrystals: Synthesis, Characterization, Physical Properties, and Applications. *Prog. Inorg. Chem.* **2005**, *54*, 47−126.
(26) Bukaluk, A.; Trzcinski, A.; Firszt, F.; Legowski, S.; Meczynska, H. Auger depth profile analysis and photoluminescence investigations of $Zn_{1-x}Mg_xSe$ alloys. *Surf. Sci.* **2002**, *507−510*, 175−180.
(27) Geng, B. Y.; You, J. H.; Zhan, F. M.; Kong, M. G.; Fang, C. H. Controllable Morphology Evolution and Photoluminescence of ZnSe Hollow Microspheres. *J. Phys. Chem. C* **2008**, *112*, 11301−11306.
(28) Liu, M.; Kitai, A. H.; Mascher, P. Point defects and luminescence centres in zinc oxide and zinc oxide doped with manganese. *J. Lumin.* **1992**, *54*, 35−42.
(29) Biswas, S.; Kar, S.; Chaudhuri, S. Optical and Magnetic Properties of Manganese-Incorporated Zinc Sulfide Nanorods Synthesized by a Solvothermal Process. *J. Phys. Chem. B* **2005**, *109*, 17526−17530.
(30) Kar, S.; Biswas, S. White Light Emission from Surface-Oxidized Manganese-Doped ZnS Nanorods. *J. Phys. Chem. C* **2008**, *112*, 11144−11149.
(31) Kloepfer, J. A.; Bradforth, S. E.; Nadeau, J. L. Photophysical Properties of Biologically Compatible CdSe Quantum Dot Structures. *J. Phys. Chem. B* **2005**, *109*, 9996−10003.
(32) Zhong, Y.; Djurisic, A. B.; Hsu, Y. F.; Wong, K. S.; Brauer, G.; Ling, C. C.; Chan, W. K. Exceptionally Long Exciton Photoluminescence Lifetime in ZnO Tetrapods. *J. Phys. Chem. C* **2008**, *112*, 16286−16295.
(33) Schubert, E. F. *Light-Emitting Diodes*, 2nd ed.; Cambridge University Press: Cambridge, U.K., 2006.